33rd Annual International Conference of the IEEE EMBS
Boston, Massachusetts USA, August 30 - September 3, 2011

An extended registration framework for the triple registration of IBZM SPECT, DATSCAN SPECT and MRI brain images to support the evaluation of brain dopamine receptor scintigraphies

Laszlo Papp, Norbert Zsoter, Peter Bandi, Sandor Barna, Ulf Luetzen

Abstract— **An extended registration model is presented to register medical image triples acquired for brain dopamine receptor scintigraphies. The model operates with rigid and non-linear transformations in parallel, where all transformation parameters are optimized by one optimization method. The concept of the transformation-sampling-similarity measurement minimizes the memory usage of a real implementation. A partial-fine sampling method is proposed to decrease the processing time of the registration. Real medical data was collected to compare our method with well-known prior ones. The first tests show that the model outperforms the classic registration methods in both speed and accuracy.**

I. INTRODUCTION

Brain dopamine receptor scintigraphies are common procedures in the daily routine of nuclear medicine [1], [3], [4], [5]. These methods provide information about receptor densities to differentiate Parkinson's disease from Parkinson's syndromes [3], [7] as well as Alzheimer's disease form Lewy-body dementia [2], [4], [5], [6]. The scintigraphies are generally performed by a Datscan (or FP-CIT) SPECT (Single Photon Emission Computed Tomography) and an IBZM SPECT acquisition representing pre-synaptic and post-synaptic events respectively [8]. The comparison of these image pairs provides metabolic information to differentiate the above diseases. Since the spatial resolution of SPECT is generally poor and does not provide morphological information, an additional MRI (Magnetic Resonance Imaging) brain acquisition is also essential for perfect localization [9], [10]. The SPECTs and the MRI are never performed at the same due to the lack of human SPECT-MRI hybrid cameras. Based on the above reasons registration is an essential step to fuse these image triples.

Brain itself is a rigid organ, hence SPECT images can be superimposed with a rigid transformation, although MRI scans may produce non-linear distortions [11]. Prior methods have shown that an extended registration of more than two images is a logical way to minimize the global misalignment of the images [12], [13], [14]. Nevertheless these methods have not taken into account that the nature of the misalignment may be different of all involved images. Furthermore the increasing number of images requires more sophisticated speed optimization methods during the registration.

We had two goals with current research: to design a fully flexible extended registration framework which minimizes a similarity function accepting rigid and non-linear transformation parameters in parallel and to apply it to the above real clinical data. The model was designed to operate with one optimization method to achieve a global optima among the images. Additionally a partial fine sampling method (PF) was introduced to decrease processing speed. The model performed the transformation, the sampling and the similarity measurement on an "atomic" level, hence no hard copy of the input images was necessary. This way it needed minimal memory.

II. MATERIALS AND METHODS

A. Patient images

18 anonymized and reconstructed DICOM (Digital Imaging and Communication in Medicine) brain MRI, IBZM SPECT and Datscan SPECT image triples were collected about patients examined by dopamine receptor scintigraphy. The average voxel resolution of the SPECT images was uniformly 4mm in axial, sagittal and coronal direction. The axial matrix size was 128x128 pixels. The MRI images had 1.0x1.0x3.0 mm voxel resolution with 512x512 axial matrix size.

B. Methods

1) Registration model: Let us denote the set of images $I = \{I_0, \ldots, I_{n-1} | n \geq 2\}$ where I_0 is the reference of the registration, and all other images are floating ones. Let $T = \{T_1, \ldots, T_{n-1}\}$ denote a transformation set, where T_i holds the corresponding transformation for I_i image. By the perspective of the current model the type of transformation is negligible.

Let $bb : (I_i, T_i) \rightarrow (\mathbb{R}^3, \mathbb{R}^3)$ bounding box function determine the minimal ($\overline{start}$) and maximal ($\overline{end}$) spatial coordinate of an I_i image by applying a T_i transformation as $(\overline{start}, \overline{end}) = bb(I_i, T_i)$. In case of the reference image T_0 is considered to be an identical transformation.

Assuming that $I_i \in I$ is a 3D image, $\overline{x} \in \mathbb{R}^3$ global coordinate provides a gray value $g \in \mathbb{R}$ from image I_i by considering the given T_i transformation and the actual bounding box values as defined by (1).

L. Papp, N. Zsoter and P. Bandi are with Mediso Medical Imaging Systems Ltd, Baross str. 91-95, Budapest, Hungary laszlo.papp@mediso.hu

S. Barna is with Scanomed Ltd., Debrecen, Hungary sandor.barna@scanomed.hu

U. Luetzen is with Medical University of Kiel, Department of Nuclear Medicine, Kiel, Germany uluetzen@nuc-med.uni-kiel.de

$$g = \begin{cases} I_i(T_i(\overline{x})) & \text{if } bb(I_i,T_i).\overline{start} < \overline{x} < bb(I_i,T_i).\overline{end} \\ min(I_i) & \text{otherwise} \end{cases} \quad (1)$$

The chosen interpolation method applied at the sampling step is not taken into account by current model.

The model is able to execute registrations after each other with different sampling parameters, where every registration execution applies several iterations to optimize all unknown $T_i \in T$ transformations. Let us denote $RE = \{re_1, \ldots, re_k\}$ iteration set which contains the maximum number of iterations for each $re_i \in RE$ registration execution.

The sampling of the images during the transformation search is performed over parallel planes in axial, sagittal and coronal direction. To characterize the distance of the planes a $PD = \left\{\overline{pd}_1, \ldots, \overline{pd}_k\right\}$ set is defined where $(\overline{pd}_i \in \mathbb{R}^3_{>0})$ represents the plain distances in the i^{th} registration execution in axial, sagittal and coronal directions. Furthermore $PS = \{\overline{ps}_1, \ldots, \overline{ps}_k\}$ set is defined where $(\overline{ps}_i \in \mathbb{R}^3_{>0})$ represents the sampling density on the planes in the i^{th} registration execution.

Let us define a $\overline{w^{fl}} = rs(I,T,\overline{x})$ resampling space function where I is the image set, T is an actual transformation set and $\overline{x} \in \mathbb{R}^3$ is a global coordinate. The result $\overline{w^{fl}} \in \mathbb{R}^{n-1}$ is a vector where $w_i^{fl} \in \overline{w^{fl}} | w_i^{fl} = I_i\left(T_i(\overline{x})\right)$ represents the sampled value from I_i floating image at $T_i(\overline{x})$ and $1 \leq i \leq n-1$. Note that the reference values never change during one registration execution since the reference image does not have a corresponding T_0 transformation (or it is considered to be identical). This way the sampling of I_0 is simply performed by $w^{ref} = I_0(\overline{x})$.

To cache the spatial coordinates that need to be transformed for sampling, let us define a SC_T sampling coordinate set based on (2)

$$\forall \overline{x} |\ sc(ps_i, pd_i, bb(I,T), \overline{x}) = true : SC_T \cup \overline{x} \quad (2)$$

where $\overline{ps_i} \in PS$ and $\overline{pd_i} \in PD$. Assuming that $\overline{ps_i} = (s_1, s_2, s_3)$, $\overline{pd_i} = (d_1, d_2, d_3)$, $\overline{x} = (x, y, z)$ and $\left\{\frac{a}{b}\right\}_0 \equiv (a \bmod b = 0)$, the definition of sc is given by (3).

$$\begin{aligned} &sc\left((s_x,s_y,s_z),(d_x,d_y,d_z),bb(I,T),(x,y,z)\right) = \\ &\Bigg(\Bigg(\left\{\frac{x}{d_1}\right\}_0 \wedge \left\{\frac{y}{d_2}\right\}_0 \wedge \left\{\frac{z}{s_3}\right\}_0\Bigg) \vee \\ &\Bigg(\left\{\frac{x}{d_1}\right\}_0 \wedge \left\{\frac{y}{s_2}\right\}_0 \wedge \left\{\frac{z}{d_3}\right\}_0\Bigg) \vee \\ &\Bigg(\left\{\frac{x}{s_1}\right\}_0 \wedge \left\{\frac{y}{d_2}\right\}_0 \wedge \left\{\frac{z}{d_3}\right\}_0\Bigg)\Bigg) \wedge \\ &\left(bb(I,T).\overline{start} < (x,y,z) < bb(I,T).\overline{end}\right) \end{aligned} \quad (3)$$

Based on SC_T the values of $I_0\left(\overline{x}\right)$ can be pre-cached in all $re_i \in RE$ registration step as defined by (4).

$$\forall w^{ref} = I_0(\overline{x}) | \overline{x} \in SC_T : SV^{ref} \cup (w^{ref}, \overline{x}) \quad (4)$$

This way SV^{ref} holds all sampled w^{ref} values and their corresponding $\overline{x}$ coordinates in a pair. The final $\overline{v}$ vector holding both reference and floating sampled values can be stored in SV sampled value set as defined by (5).

$$\begin{aligned} &\forall \overline{x} \in SC_T : SV \cup \overline{v} = (w^{ref}, \overline{w^{fl}}) | \\ &(w^{ref}, \overline{x}) \in SV^{ref}, \overline{w^{fl}} = rs(I,T,\overline{x}) \end{aligned} \quad (5)$$

Let us denote an $sm : \mathbb{R}^n \to \mathbb{R}$ similarity measurement function which measures the similarity value $\delta \in \mathbb{R}$ based on all sampled $\overline{v} \in SV$ by $\delta = sm(SV)$. Note that the way of transformation, sampling and similarity measurement does not require the transformed hard copy of the original images, furthermore the reference values are cached in all registration execution step. Let om refer to an optimization method which can get a δ similarity value and return with a new T transformation set. Over the iterations om minimizes the δ similarity value which is associated with the optimal T transformation.

Based on the above definitions the algorithm of the registration framework is defined as Tab. I.

2) Medical Application: The above model was the base of current triple registration where sm was an extended normalized mutual information [14] defined as (6), and om was the Downhill-Simplex method [15].

$$-\frac{H(I_0) + H(I_1) + H(I_2)}{H(I_0, I_1, I_2)} \quad (6)$$

where $H(I_i)$ $(0 \leq i \leq 2)$ was the Shannon entropy [16] of image I_i as defined by (7) and $H(I_0, I_1, I_2)$ was the joint Shannon entropy of images I_0, I_1 and I_2 as defined by (8).

$$H(I_i) = -\sum_{a \in I_i} p(a) \log p(a) \quad (7)$$

where $p(a)$ is the probability of a value occurrence in image I_i.

$$H(I_0, I_1, I_2) = -\sum_{a \in I_0} \sum_{b \in I_1} \sum_{c \in I_2} p(a,b,c) \log p(a,b,c) \quad (8)$$

where $p(a,b,c)$ is the probability of the mutual a, b, c value occurrence in images I_0, I_1 and I_2 respectively.

For settings of RE,PD,PS and the type of $T_i \in T$ see Tab. II.

The $I_0, I_1, I_2 \in I$ images were considered as the Datscan SPECT, MRI and the IBZM SPECT Respectively. Overall,

TABLE II

PARAMETERS OF THE REGISTRATION FRAMEWORK TO REGISTER THE MRI AND IBZM SPECT TO THE DATSCAN SPECT

i	$\overline{re_i}$	$\overline{pd_i}$ (mm)	$\overline{ps_i}$ (mm)	Type of T_1	Type of T_2
1	200	(64,64,64)	(32,32,32)	rigid	rigid
2	200	(32,32,32)	(8,8,8)	rigid	rigid
3	500	(16,16,16)	(4,4,4)	nonlinear	rigid

Current settings assume that the reference image was the Datscan SPECT, furthermore T_1 and T_2 were the transformations for the MRI and the IBZM SPECT respectively.

TABLE I

MAIN STEPS OF THE EXTENDED REGISTRATION FRAMEWORK

1	$I := \{I_0, \ldots, I_{n-1}\}$	Declare I image set
2	$T := \{T_1, \ldots, T_{n-1}\} \mid T_i = id$	Declare T as the set of identical transformations
3	$RE := \{\overline{re_1}, \ldots, \overline{re_k}\}$	Declare the registration execution set
4	$PD := \left\{\overline{pd}_1, \ldots, \overline{pd}_k\right\}$	Declare the plain distances set
5	$PS := \{\overline{ps}_1, \ldots, \overline{ps}_k\}$	Declare the plain sampling set
6	$\forall 1 \leq i \leq k:$	Go through registration executions
7	$SC_T := \oslash$	Initialize the sampling coordinate set
8	$\forall \overline{x} \mid\ sc(\overline{ps_i}, \overline{pd_i}, bb(I,T), \overline{x}) = true : SC_T \cup \overline{x}$	Calculate the actual sampling coordinates and collect them into SC_T set
9	$SV^{ref} := \oslash$	Initialize the cached reference value-coordinate pair set.
10	$\forall w^{ref} = I_0(\overline{x}) \mid \overline{x} \in SC_T : SV^{ref} \cup (w^{ref}, \overline{x})$	Collect the pair of the sampled reference w^{ref} value and its $\overline{x}$ coordinate
11	$\forall 1 \leq j \leq re_i:$	Go through optimization iterations
12	$SV := \oslash$	Initialize the sampled values set
13	$\forall \overline{x} \in SC_T:$	Go through the $\overline{x}$ sample coordinates
14	$\overline{w^{fl}} := rs(I, T, \overline{x})$	Calculate the actual $\overline{w^{fl}}$ value vector which holds the values of the floating images
15	$\overline{v} := (w^{ref}, \overline{w^{fl}}) \mid (w^{ref}, \overline{x}) \in SV^{ref}$	Append the pre-calculated w^{ref} and the corresponding $\overline{w^{fl}}$ values to $\overline{v}$
16	$SV \cup \overline{v}$	Collect $\overline{v}$ into SV
17	$\delta := sm(SV)$	Calculate the similarity value based on actual SV
18	$T := om(\delta)$	Generate a new T by om optimization method based on δ similarity value

3 registration executions were performed. The first two executions optimized T_1, and T_2 by rigid transformations, hence om had to minimize 12 parameters (6-6 parameters for shifting and rotation for both floating images). The last execution optimized a nonlinear b-spline transformation [12] for I_1 and a rigid one for I_2. The control points of the non-linear transformation were the intersections of pd_1 planes (see Tab. II).

C. Validation

In order to compare our method to prior proposed ones, the registration of the image triples was performed by two classic dual NMI based non-linear and rigid registrations between $I_0 - I_1$ and $I_0 - I_2$ pairs respectively. In these cases the values of $\overline{re_i}$ were the same as shown in Tab. II. To compare our partial fine strategy to classic ones, the two dual NMI registrations took samples regularly based on the values of $\overline{ps_i}$. Since the misalignments of the medical image triples were unknown, the validation of our method in these cases was performed by visual inspection.

Due to the above limitations an automated validation was performed as well based on simulated data. Two artificial SPECT images were created from all real MRI images. The resolution of the artificial SPECT images was decreased to the level of the original SPECT ones and the voxel values were smoothed by direct neighbor values. A known rigid and non-linear transformation was applied to the artificial IBZM SPECT, and the MRI respectively.

To compare our partial-fine sampling strategy to regular ones, our method was also applied with $\overline{pd_i} = \overline{ps_i}$ settings in both real and simulated cases.

The mean and standard deviation of the rigid and non-linear parameter differences were calculated for all three methods.

TABLE III

TRANSFORMATION PARAMETER ERRORS ON REAL IMAGES

	T_1 non-linear error	T_2 rigid error
Our method	2.3512± 0.8543	0.9324 ± 1.1349
Our method (PF)	2.5627± 1.5291	1.1853 ± 1.3581
dual NMI	3.8396± 2.3466	1.9767 ± 1.9248

Cells represent $\mu \pm \sigma$ values in mm.

TABLE IV

TRANSFORMATION PARAMETER ERRORS ON SIMULATED IMAGES

	T_1 non-linear error	T_2 rigid error
Our method	2.1158± 0.9576	0.6314 ± 0.8198
Our method (PF)	2.2013± 1.2745	0.8701 ± 0.9543
dual NMI	2.4396± 1.2243	0.9677 ± 0.9732

Cells represent $\mu \pm \sigma$ values in mm.

III. RESULTS

Based on Tab. III and Tab. IV, our method outperformed the dual NMI registration with both regular and partial fine sampling strategies. Our PF strategy was slightly less accurate than our regular one, although the latter one needed much more computation. The average time of our method was $25sec$ applying PF strategy and $134sec$ applying regular sampling. The sum of the registration time of the two dual registrations was $112sec$.

IV. CONCLUSIONS AND FUTURE WORKS

A. Conclusions

We have presented a registration framework which is able handle different transformations for different floating images. This way the global optima can be achieved by one extended registration. Although our method outperformed the classic

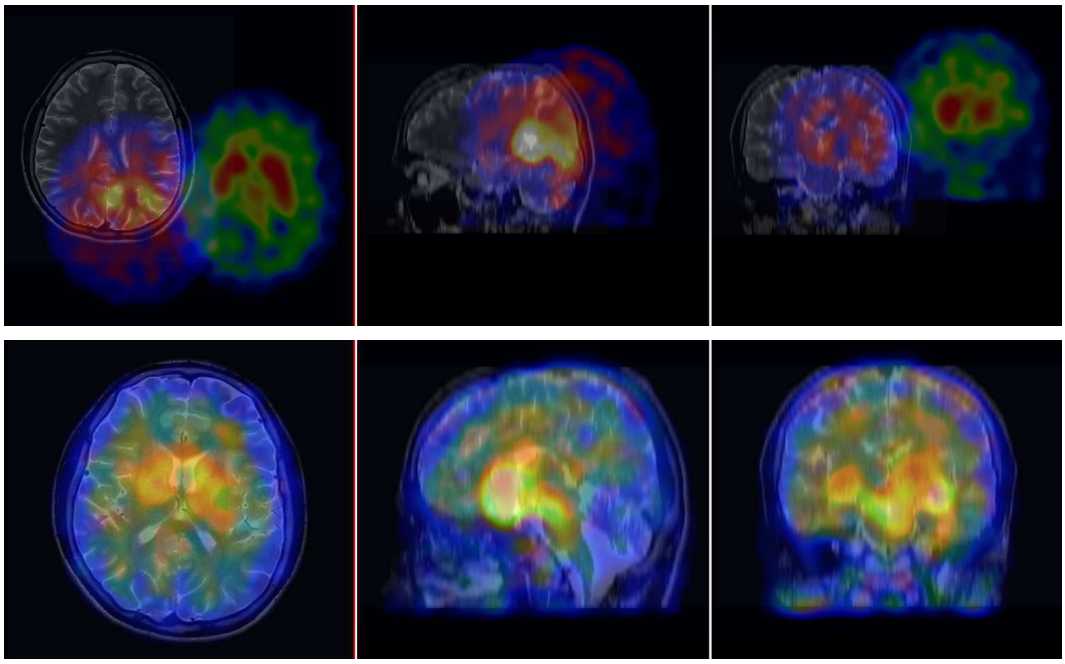

Fig. 1. A real medical IBZM SPECT-Datscan SPECT-MRI example representing the initial stage (top) and the result provided by our framework applying the PF sampling strategy (bottom).

registration with both regular and PF sampling strategies, it also had an increased computational complexity. Considering that our PF sampling strategy did not decrease the accuracy of the registration significantly, but significantly decreased the processing speed, it is advised to be involved in future extended registration techniques.

B. Future Works

Current framework will be tested on images acquired about neuro-endocrine tumors to support decision making in the therapy [17]. Our framework will be further developed to operate with image groups where one group can be superimposed by one transformation. This situation appears when follow-up multi-modal studies are acquired by a hybrid camera. This way much more images could be involved into the framework without increasing the number of unknown transformations.

REFERENCES

[1] P. Rmy, Z. Malek, E. Itti, 123I-Ioflupane brain scintigraphy (DaTScan) to demonstrate loss of nigrostratal dopaminergic neurons: principles and applications, *Rev Neurol*, vol. 159, 2003, pp. 942-946.

[2] E. Donnemiller, J. Heilmann, G. K. Wenning, et al., Brain perfusion scintigraphy with 99mTc-HMPAO or 99mTc-ECD and 123I--CIT single-photon emission tomography in dementia of the Alzheimer-type and diffuse Lewy body disease, *Eur J Nucl Med Mol Img*, vol. 24, 1997, pp. 320-325.

[3] J. Spiegel, M.-O. Mllers, W. H. Jost, et al., FP-CIT and MIBG scintigraphy in early Parkinson's disease, *Movement Disorders*, vol. 20, 2005, pp. 552-561.

[4] H. Hanyu, S. Shimizu, K. Hirao, et al., Comparative value of brain perfusion SPECT and [123I]MIBG myocardial scintigraphy in distinguishing between dementia with Lewy bodies and Alzheimers disease, *Eur J Nucl Med*, vol. 33, 2006, pp. 248-253.

[5] I. G. McKeith, D. W. Dickson, J. Lowe, et al., Diagnosis and management of dementia with Lewy bodies, *Neurology*, vol. 65, 2005, pp. 1863-1872.

[6] J. T. O'Brien, S Colloby, J. Fenwick, Dopamine Transporter Loss Visualized With FP-CIT SPECT in the Differential Diagnosis of Dementia With Lewy Bodies, *Arch Neurol*, vol. 61, 2004, pp. 919-925.

[7] T. S. Hani, J. Patterson, D. J. Wyper, Correlation of Parkinson's disease severity and duration with 123I-FP-CIT SPECT striatal uptake, *Movement Dosirders*, vol. 15, 2000, pp. 692-698.

[8] C. C. P. Verstappen, B. R. Bloem, C. A. Haaxma, et al., Diagnostic value of asymmetric striatal D2 receptor upregulation in Parkinsons disease: an [123I]IBZM and [123I]FP-CIT SPECT study, *Eur J Nucl Med Mol Img*, vol. 34, 2007, pp. 502-507.

[9] C. Scaglione, A. Ginestroni, A. Vella, et al., MRI and SPECT of midbrain and striatal degeneration in fragile X-associated tremor/ataxia syndrome, *J Neurology*, vol. 255, 2008, pp. 144-146.

[10] R. J. Clifford, M. A. Bernstein , N. C. Fox, The Alzheimer's disease neuroimaging initiative (ADNI): MRI methods, *J Magn Res Imag*, vol. 27, 2008, pp. 685-691.

[11] F. M. Bui, K. Bott, M. P. Mintchev, A quantitative study of the pixel-shifting, blurring and nonlinear distortions in MRI images caused by the presence of metal implants, *J Med Eng Tech*, vol. 24, 2000, pp. 20-27.

[12] S. K. Balci, P. Golland, M. Shenton, et al., Free-Form B-spline Deformation Model for Groupwise Registration, *Med Image Comput Comput Assist Interv, MICCAI*, vol. 10, 2007, pp. 23-30.

[13] C. Wachinger, N. Navab, Structural image representation for image registration, *2010 IEEE Computer Society Conference on Computer Vision and Pattern Recognition Workshops (CVPRW)*, 2010, pp. 23-30.

[14] L. Papp, N. Zsoter, G. Szabo, et al., Parallel registration of multi-modal medical image triples having unknown inter-image geometry, *Annual International Conference of the IEEE Engineering in Medicine and Biology Society, EMBC 2009*, 2009, pp. 5825 - 5828.

[15] J.L Bernon, V Boudousqa, J.F Rohmer, et al., A comparative study of Powell's and Downhill Simplex algorithms for a fast multimodal surface matching in brain imaging, *Comp Med Img Graph*, vol. 25, 2001, pp. 287-297.

[16] J. P. W. Pluim, J. B. A. Maintz, M. A. Viergever, et al., Mutual-information-based registration of medical images: a survey, *IEEE Transactions on Medical Imaging*, vol. 22, 2003, pp. 986 - 1004.

[17] G. Kaltsas, A. Rockall, D. Papadogias, Recent advances in radiological and radionuclide imaging and therapy of neuroendocrine tumours, *Eur J Endocr*, vol. 151, 2004, pp. 15-27.